http://dx.doi.org/10.5012/bkcs.2013.34.3.793

Effect of Foreign Molecules on the SERS of Probe Molecules Trapped in Gaps between Planar Ag and Nano-sized Ag Particles

Kwan Kim,* Jeong-Yong Choi, and Kuan Soo Shin†,*

*Department of Chemistry, Seoul National University, Seoul 151-742, Korea. *E-mail: kwankim@snu.ac.kr*
*†Department of Chemistry, Soongsil University, Seoul 156-743, Korea. *E-mail: kshin@ssu.ac.kr*
Received October 29, 2012, Accepted December 11, 2012

A few years ago, the plasmon-induced electronic coupling (PIEC) model was proposed in the literature to explain small changes in the surface-enhanced Raman scattering (SERS) in nanogap systems. If this model is correct, it will be very helpful in both basic and application fields. In light of this, we carefully reexamined its appropriateness. Poly(4-vinylpyridine) (P4VP) used in the earlier work was, however, never a proper layer, since most adsorbates not only adsorbed onto Ag nanoparticles sitting on P4VP but also penetrated into the P4VP layer deposited initially onto a flat Ag substrate, ultimately ending up in the SERS hot sites. Using 1,4-phenylenediisocyanide and 4-nitrophenol as the affixing layer and the foreign adsorbate, respectively, we could clearly reveal that the PIEC model is not suited for explaining the Raman signal in a nanogap system. Most of the Raman signal must have arisen from molecules situated at the gap center.

Key Words : Surface-enhanced Raman scattering, Plasmon-induced electronic coupling, Poly(4-vinylpyridine), Nanoparticle, Nanogap

Introduction

Noble metallic nanostructures exhibit a phenomenon known as surface-enhanced Raman scattering (SERS) in which the scattering cross sections are dramatically enhanced for molecules adsorbed thereon.[1-3] In recent years, it has been reported that even single-molecule spectroscopy is possible using SERS, suggesting that the enhancement factor (EF) can reach as much as 10^{14}-10^{15}.[2,4-7] In this case, the effective Raman cross sections are comparable to the usual fluorescence cross sections. SERS has thus been applied in many areas of science and technology, including surface chemical analysis, electrochemistry, chemical or biomolecular sensing, and molecular electronics.[8-12] In contrast, however, the origin of SERS has not yet been fully clarified, although electromagnetic and chemical enhancement mechanisms are definitely crucial.[13-15] It has generally been accepted that at least 8-10 orders of magnitude of enhancement can arise from electromagnetic surface plasmon excitation, in addition to the chemical enhancement associated with either the metal-to-molecule or the molecule-to-metal charge transfer transition.[5,16]

Besides the electromagnetic and chemical enhancement mechanisms, Chumanov and coworkers proposed few years ago that SERS can also occur *via* plasmon-induced electronic coupling (PIEC) between the oscillating electrons in the metal and the electronic system of the adsorbed molecules.[17,18] In this model, because of the excitation of the plasmon resonances, the oscillating electrons in the metal can penetrate the electronic system of the adsorbed molecules, inducing strong molecular polarization. This mechanism was claimed to be able to account for the two typical features of SERS: its dependence on the chemical nature of the molecules and its requirement of plasmon resonances. This mechanism was proposed on the basis of SERS spectral data gathered using substrates composed of silver nanoparticle arrays on silver mirror films (NAMF). Initially, the immobilization was accomplished with, for instance, a poly(4-vinylpyridine) (P4VP) layer that strongly binds to the surface of both the Ag mirror film and the Ag nanoparticles *via* the nitrogen atom on the pyridine ring. It was expected that the additional exposure of the NAMF substrates to the same molecules (*e.g.*, P4VP) would yield more SERS signal; however, no increase in the SERS signal was detected, despite the greater amount of molecules adsorbed on top of the Ag nanoparticles. A surprising observation was made when dissimilar molecules were adsorbed on the NAMF substrates: the SERS signal from the affixing layer (*e.g.*, P4VP) was partially or completely quenched and the degree of quenching was dependent on the chemical nature of the adsorbed molecules and the molecules used for the affixing layer. Since the latter observation was difficult to explain within the framework of the usual electromagnetic and chemical enhancement mechanisms, a different mechanism for SERS was proposed based on PIEC.

We have recently estimated the apparent size of the "hot site" for SERS located within the gap between two spherical Au nanoparticles.[19] Initially, 55-nm sized Au nanoparticles were laid on a thiol-group-terminated silane film, and then 1,4-phenylenediisocyanide (1,4-PDI) molecules were self-assembled onto the Au nanoparticles. 1,4-PDI bonded to Au by forming one Au-CN bond so that another isocyanide group is pendent with respect to the Au surface. Up to this point, no Raman scattering was detected at all for 1,4-PDI. When new Au nanoparticles were attached to the pendent isocyanide groups of 1,4-PDI, a Raman signal was distinctly

observed. This can be understood in terms of the electromagnetic "hot sites" formed at the gaps between two Au nanoparticles.[20,21] The Raman signal did not increase further, however, even after the adsorption of additional 1,4-PDI onto the vacant surfaces of the second group of Au nanoparticles. This is consistent with the observation of Chumanov *et al.* that the additional exposure of the NAMF substrates to the same molecules did not yield more SERS signal, suggesting that the size of hot site is in fact very limited. Although it was not reported, the SERS spectral pattern of 1,4-PDI was not affected at all in our system even when dissimilar molecules were adsorbed on the surfaces of the second group of Au nanoparticles. This observation obviously conflicts with the PIEC model proposed by Chumanov et al. We have thus reexamined the SERS characteristics of NAMF systems using P4VP as the affixing layer between a flat Ag surface and Ag nanoparticles and concluded that P4VP is not a proper layer for experiments supporting the PIEC model, since most molecules that adsorb on Ag not only adsorb on Ag nanoparticles but also penetrate into the P4VP layer, ultimately ending up in the SERS hot sites.

Experimental Section

Silver nitrate ($AgNO_3$), trisodium citrate ($C_6H_5O_7Na_3$), 4-mercaptobenzoic acid (4-MBA), 4-aminobenzenethiol (4-ABT), 4-mercaptophenol (4-MPh), 4-nitrophenol (4-NP), and P4VP (MW 160 kDa) were purchased from Aldrich and used as received. Other chemicals, unless specified, were reagent grade, and highly purified water with a resistivity greater than 18.0 MΩ·cm (Millipore Milli-Q System) was used in preparing the aqueous solutions.

Ag hydrosol was prepared by following the modified recipes of Lee and Meisel.[22] Initially, 100 mL of 1 mM aqueous solution of $AgNO_3$ was heated to boiling, and then 2 mL of 1% (w/v) aqueous solution of trisodium citrate was added. After it was boiled for 1 h, the mixture was allowed to cool while still being stirred. For the adsorption experiment, the sol was diluted 10 times with water. A macroscopically smooth Ag substrate was prepared by resistive evaporation of titanium and silver at 1×10^{-6} Torr onto a freshly cleaved mica sheet. After deposition of silver (~200-nm thick), the evaporator was back-filled with nitrogen. Separately, a SERS-active Ag substrate was prepared by soaking an Ag foil into an (1:1) aqueous solution of HNO_3 for 30 s. P4VP films on silicon or Ag substrates were prepared by spin-casting 10 μL of ethanolic P4VP solutions of different concentrations (from 0.05 to 1 wt %) at 3000 rpm for 30 s.

The zeta potential of the Ag nanoparticles was measured in a Malvern Zetasizer 3000HS (Malvern Instruments). UV-visible (UV-vis) spectra were obtained with a SCINCO S-4100 spectrometer. Transmission electron microscopy (TEM) images were acquired using a JEM-200CX transmission electron microscope at 160 kV. Field emission scanning electron microscopy (FE-SEM) images were obtained with a JSM-6700F field emission scanning electron microscope operating at 5.0 kV. Atomic force microscopy (AFM) images were obtained with a Digital Instrument Nanoscope IIIa scanning probe microscope. Static water contact angle measurement was carried out using a Phoenix goniometer. The thickness of the P4VP films was estimated using a Rudolph Auto EL II optical ellipsometer; at least three different sampling points were considered to obtain the average thickness value. Raman spectra were obtained using a Renishaw Raman system Model 2000 spectrometer equipped with an integral microscope (Olympus BH2-UMA). The 632.8 nm line from a 17 mW He/Ne laser (Spectra Physics model 127) was used as the excitation source. Raman scattering was detected over 180° using a Peltier-cooled (−70 °C) charge-coupled device camera (400 × 600 pixels). The laser beam was focused on a spot approximately 1 μm in diameter with an objective microscope with a magnification on the order of 20×. The holographic grating (1800 grooves/mm) and the slit provided a spectral resolution of 1 cm^{-1}. The Raman band of a silicon wafer at 520 cm^{-1} was used to calibrate the spectrometer.

Results and Discussion

Figure 1(a) shows a TEM image of the Ag sol particles prepared in this work. Most of the nanoparticles were spherical in shape, with a mean diameter of 75 ± 15 nm: see Figure 1(b) for the size distribution histogram of Ag nanoparticles. On the other hand, these Ag particles exhibited a very distinct surface plasmon absorption band at 435 nm, as shown in Figure 1(c). According to a zeta-potential measurement, the Ag nanoparticles were negatively charged (–47.9 mV), probably because of citrate ions adsorbed onto them. Because of the electrostatic repulsion of the negatively charged Ag nanoparticles, we did not expect the surface coverage of Ag nanoparticles adsorbed onto the affixing layer (*e.g.*, P4VP) to be large (vide infra).

We have measured the thicknesses of P4VP films produced by spin-casting: 10 μL of ethanolic P4VP solution was spin-cast onto a silicon wafer at 3000 rpm. Figure 2 shows the ellipsometric thickness of the film as a function of the P4VP concentration. The thickness is found to increase linearly with P4VP concentration. When 0.2 wt % solution was spin-cast, the thickness was measured to be ~10 nm, but when the concentration was increased to 1 wt %, it became as thick as 65 nm. Separately, the thickness of a P4VP film spin-cast similarly onto an Ag film using a 1 wt % P4VP solution was measured to be 65 nm. Although the ellipsometric data for P4VP on a metal substrate might be less reliable than those obtained on a dielectric substrate, these results indicate that much the same P4VP film likely was assembled on an Ag film as on a silicon wafer. This is not unreasonable, since the static contact angle of a clean Ag film (63.9°) is close to that of a silicon wafer (64.5°).[23,24] At any rate, precise thickness adjustment is unnecessary in this work, so we have prepared P4VP films on Ag simply by referring to the thickness data in Figure 2.

The Ag film produced by vacuum evaporation onto a mica sheet was very smooth: an AFM image showed that the Ag surface was composed of atomically flat terraces spanning

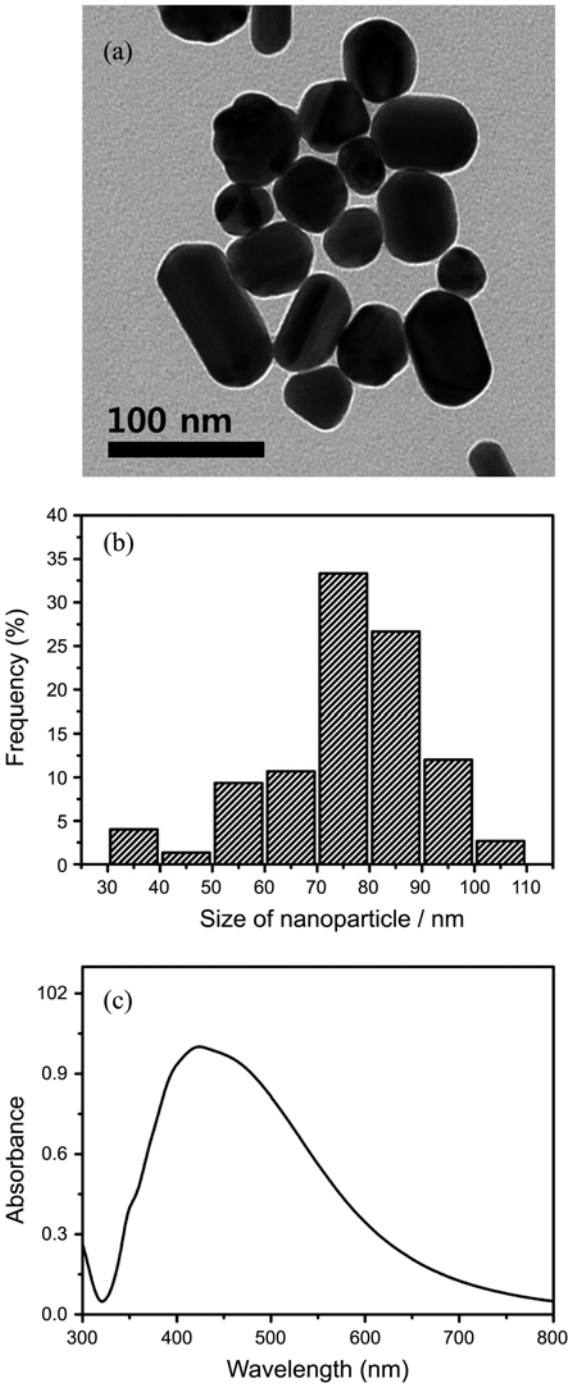

Figure 1. TEM image, (b) particle size distribution histogram, and (c) UV-vis extinction spectrum of Ag nanoparticles.

several hundred nm in size.[25] After spin-casting P4VP on the vacuum-evaporated Ag film, we examined how effectively Ag nanoparticles could bind to P4VP by soaking it in aqueous Ag sol for 1 h. Figure 3(a) shows a typical FE-SEM image taken after the adsorption of Ag nanoparticles onto the surface of P4VP coated on a vacuum-evaporated Ag film; the system can be denoted as Ag@P4VP/Ag(flat). It is seen that, on average, 11 Ag nanoparticles were bound per 1 μm^2 area of P4VP. The surface coverage of Ag nanoparticles is not large, as a result of their electrostatic repulsion (vide

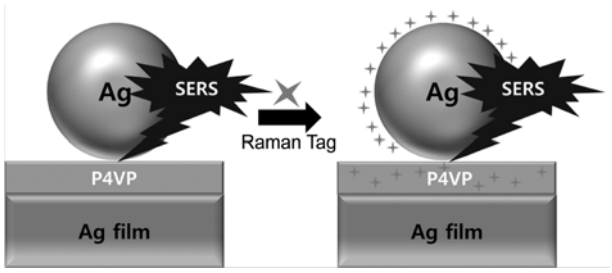

Scheme 1. Schematic diagram of the effect of foreign molecules on the SERS of probe molecules trapped in gaps between planar Ag and Ag nanoparticles.

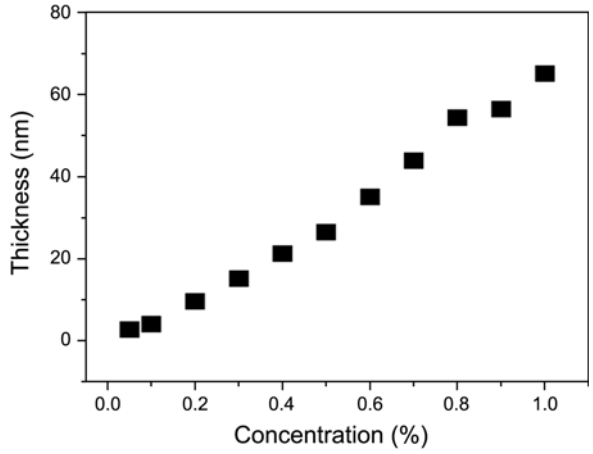

Figure 2. Ellipsometric thickness of P4VP film formed on a silicon wafer by spin-casting at 3000 rpm for 30 s.

supra). In any case, the gaps between Ag nanoparticles and the flat Ag film can function as SERS-active sites. The SERS activity must increase with decreasing gap sizes. This is evidenced in the Raman spectra shown in Figure 3(b), which are taken as a function of P4VP thickness. It should be noted that in the absence of Ag nanoparticles, we could not detect any Raman peaks, even from a 65-nm-thick P4VP film prepared by spin-casting a 1 wt % P4VP solution. The Raman peaks of P4VP were very clearly identifiable when Ag nanoparticles were deposited, even onto a P4VP film assembled using a 0.05 wt % solution (corresponding to a thickness of 2.2 nm); the assignment of Raman peaks of P4VP can be found in the literature: 1598 cm^{-1} (8a, ring stretch); 1201 cm^{-1} (9a, CH in-plane bend); 1068 cm^{-1} (18a, CH in-plane bend); 999 cm^{-1} (1, ring breathing).[26-30] However, the P4VP peaks weakened rapidly as the thickness increased, becoming barely detectable when Ag nanoparticles were bound onto a P4VP film prepared using a 0.2 wt % solution (corresponding to a thickness of 9.1 nm).

We subsequently examined the response of the P4VP nanogaps formed between a flat Ag substrate and Ag nanoparticles toward 4-ABT, 4-MBA, or 4-MPh as a function of the thickness of P4VP from 2.2 nm up to 65 nm. An appropriate amount of P4VP was first deposited onto a vacuum-evaporated Ag film on a mica sheet, and then Ag nanoparticles were adsorbed onto the exposed P4VP film. The Ag-nanoparticle-adsorbed P4VP film was cut into several

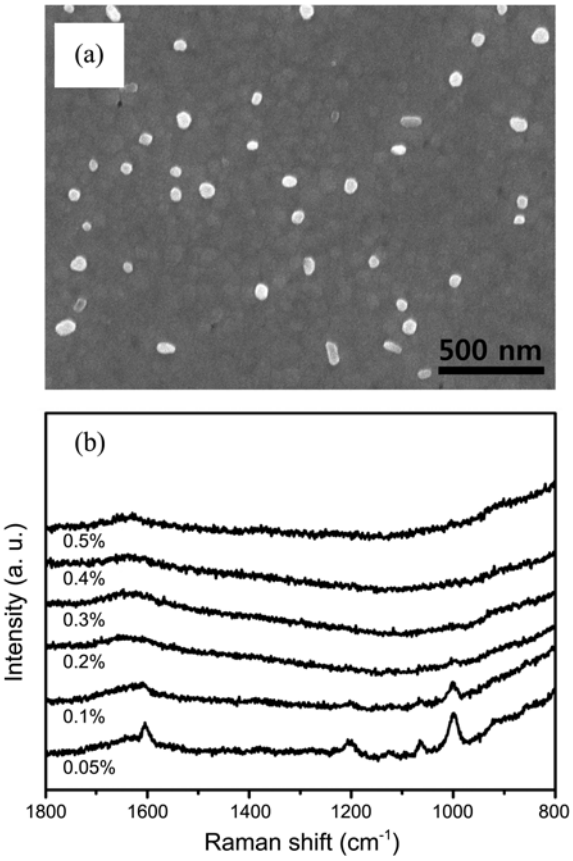

Figure 3. (a) FE-SEM image and (b) a series of Raman spectra taken after P4VP films (with different thicknesses) assembled on flat Ag substrates were soaked in an aqueous Ag sol for 1 h.

pieces, after which each piece (1 mm × 10 mm) was put into a glass capillary. Then, Raman spectra were measured as a function of time by flowing aqueous solutions of 10 μM 4-ABT, 4-MBA, or 4-MPh. Since the P4VP film was unstable in contact with ethanol, we used aqueous solutions rather than ethanolic solutions. Figure 4(a) shows a collection of Raman spectra measured under a 4-MBA flow at times of 0, 2, 4, 6, 8, 10, 30, and 60 min; all Raman intensities were normalized with respect to that of a silicon wafer at 520 cm^{-1}. The 4-MBA peaks were difficult to identify, at least within 1 h, when the thickness of P4VP was greater than 15 nm (corresponding to the 0.3 wt % spin-cast solution). However, the 4-MBA peaks were identifiable from the beginning when the thickness of P4VP was 2.2 nm (corresponding to the 0.05 wt % spin-cast solution); the SERS spectrum of 4-MBA is dominated by the strong bands at about 1587 cm^{-1} (8a, ring vibration) and 1077 cm^{-1} (12, ring vibration).[31] This can be seen more clearly in Figure 4(b), in which the Raman intensity of 4-MBA at 1587 cm^{-1} (denoted by an asterisk (*) in Figure 4(a)) is shown as a function of the flow time of 4-MBA. When the P4VP thickness was 2.2 nm, the Raman peaks of 4-MBA were saturated within 10 min. The Raman peaks of 4-MBA were similarly saturated about 10 min later when the thickness of P4VP was 3.5 nm (corresponding to the 0.1 wt % spin-cast solution). The peak intensity in this case was, however, at most 30% of that obtained from a 2.2-nm-thick film. This is not unexpected, since the SERS activity in the gap sites must decrease profoundly with increasing P4VP thickness. This assumes that all the SERS peaks in Figure 4(a) are due the chemical species present inside the gaps formed between Ag nanoparticles and the flat Ag film. Otherwise, 4-MBA peaks should be identifiable even from a film thicker than 15 nm. The Ag nanoparticles themselves did not produce any measurable Raman signal for 4-MBA adsorbed onto them.

The adsorption of 4-MBA onto Ag nanoparticles should occur immediately after the exposure of the Ag@P4VP/Ag(flat) system to the 4-MBA solution. If PIEC was the sole origin of the SERS, the Raman peaks of 4-MBA would have been saturated shortly after the flow of 4-MBA solution. Even with a 2.2-nm-thick film, it took at least 10 min for the 4-MBA peaks to become saturated. This would supposedly then indicate that the SERS peaks in Figure 4(a) are mostly due to 4-MBA and P4VP present in the gaps between Ag nanoparticles and the planar Ag film. This implies that 4-MBA could readily penetrate into the P4VP film. In this sense, we examined the robustness of the P4VP film against aromatic thiol molecules such as 4-MBA, 4-ABT, and 4-MPh. This was accomplished by measuring Raman spectra using a SERS-active Ag foil as the base substrate. Specifically, an Ag foil was soaked in a 1:1 HNO_3 solution for 30 s and washed thoroughly with water. Then, a 65-nm- thick P4VP film was spin-cast (using 1 wt % solution) thereon. The P4VP-adsorbed Ag foil was cut into several pieces (1 mm × 10 mm), and each piece was put into a glass capillary and later subjected to Raman spectral measurement under a flow of 10 μM aqueous solution of 4-MBA, 4-ABT, or 4-MPh. Figure 5(a) shows a series of Raman spectra measured every 10 minutes during the flow of 4-MBA solution. Figures 5(b) and (c) show similar Raman spectra measured during flows of 4-ABT and 4-MPh, respectively. At the beginning, we could identify only the authentic peaks of P4VP, but as time went on, the peaks of 4-MBA, 4-ABT, and 4-MPh grew rapidly. This must indicate that even a 65-nm-thick P4VP film is not rigid and robust enough to prevent the diffusion of aromatic thiol molecules to near the Ag surface. Figure 5(d) shows the growth patterns of the Raman peaks denoted by asterisks (*) in Figures 5(a)-(c) collectively; the Raman intensities were normalized with respect to the saturated values. The detailed assignments of SERS spectra of 4-ABT[32-35] and 4-MPh[36] can be found in the literatures. The P4VP peaks were dominant within 20 min, after which the peaks of 4-MBA, 4-ABT, and 4-MPh grew rapidly with almost the same rate for 2 h. It is thus expected that the Raman peaks of 4-MBA, 4-ABT, and 4-MPh will appear within a shorter time if the thickness of the P4VP is reduced. In fact, the Raman peaks of 4-MBA, 4-ABT, and 4-MPh were saturated within 10 min when the P4VP film was 2.2 nm thick (corresponding to the 0.05 wt % spin-cast solution).

We noticed in Figure 5(d) that about 2 h was needed for the Raman peaks of 4-MBA, 4-ABT, and 4-MPh to become saturated. Assuming that a Fickian diffusion model is applicable to the penetration of 4-MBA, 4-ABT, and 4-MPh into

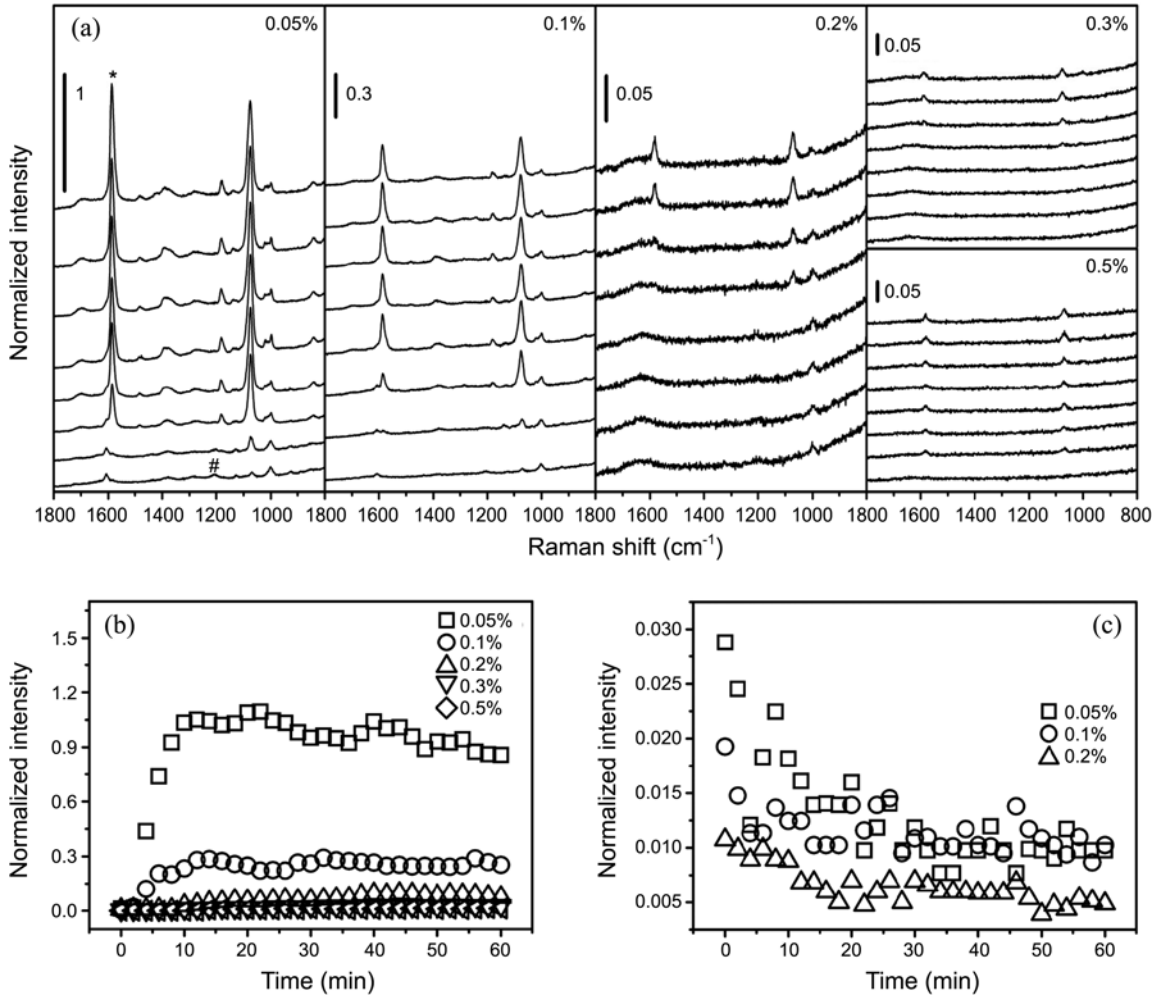

Figure 4. (a) Raman spectra measured as a function of time, *i.e*., at times of 0, 2, 4, 6, 8, 10, 30, and 60 min, under the flow of 4-MBA through capillaries containing Ag@P4VP/Ag(flat) substrates with different thicknesses of P4VP. Peak intensity of (b) 4-MBA (denoted by an asterisk (*)) and (c) P4VP (denoted by a sharp (#)) in (a) *versus* the measurement time.

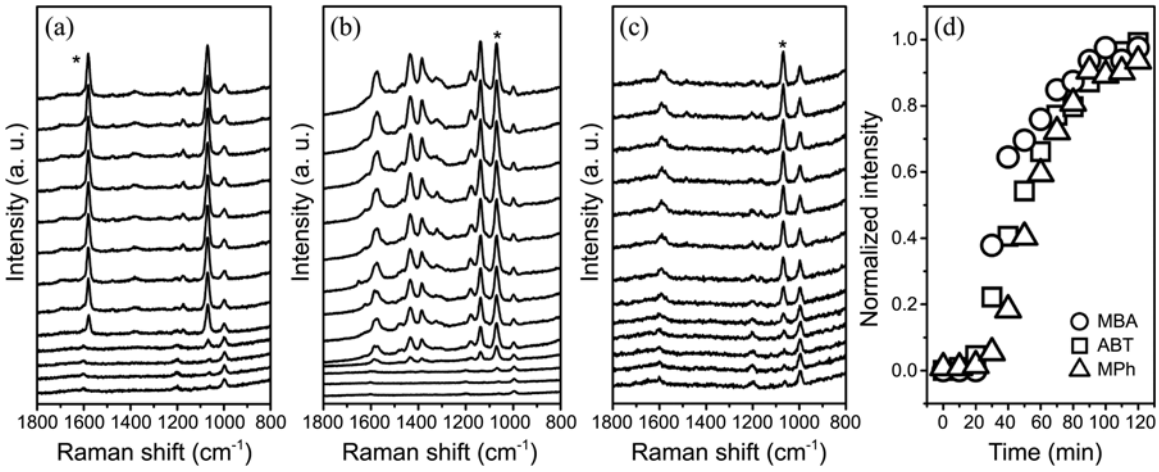

Figure 5. Series of Raman spectra measured every 10 minutes during the flow of a 10 μM aqueous solution of (a) 4-MBA, (b) 4-ABT, or (c) 4-MPh through a capillary containing a 65-nm-thick P4VP film assembled on SERS-active Ag foil (etched using HNO_3). (d) Intensity variation of peak denoted by an asterisk (*) in (a)-(c) *versus* the measurement time.

the P4VP layer, the observed data dictates that the diffusion coefficient will be on the order of 10^{-15} cm^2/s since it must be close to the thickness squared divided by the measurement-time required for saturation.[37] The reported values of diffusion coefficient in polymers at room temperature for a molecule like CCl_4 having a diameter of 0.55 nm range over many

orders of magnitude, from 10^{-7} cm^2/s in rubbery polymers (polyethylene) to 10^{-17} cm^2/s in glassy polymers (polyvinyl chloride).[38] In any case, we saw in Figure 4(b) that the Raman peaks of 4-MBA were saturated about 10 min later when 4-MBA was flowed through a capillary containing an Ag@P4VP(2.2 nm)/Ag(flat) substrate. We separately found above that about 10 min is required for 4-MBA molecules to penetrate into the 2.2-nm-thick P4VP film. This clearly supports the earlier argument that the Raman peaks in Figure 4(a) are exclusively due to 4-MBA and P4VP present in the gaps between Ag nanoparticles and the planar Ag film. It is expected that the occupation of 4-MBA molecules in the gap sites will result in a decrease in the number of P4VP molecules detectable by SERS. As can be seen in Figure 4(c), the Raman peak of P4VP at 1201 cm^{-1} (denoted by a sharp (#) in Figure 4(a)) was, in fact, weakened during the first 10-15 minutes, which is probably the time required for the saturation of 4-MBA molecules inside the gaps. Much the same observation was made using 4-ABT and 4-MPh as the probe molecules.[25] All these observations refute the PIEC model as a means to explain the occurrence of SERS.

All the thiols used above as probe molecules, *i.e.*, 4-MBA, 4-ABT, and 4-MPh, can readily adsorb on Ag nanoparticles. What will happen if the probe molecule barely adsorbs onto the Ag nanoparticles? To see what will happen, we have chosen 4-NP, which hardly adsorbs on Ag, as a probe molecule. After a nanogap system composed of 75-nm-sized Ag nanoparticles, 2.2-nm-thick P4VP film, and a flat Ag substrate was fabricated (Ag@P4VP(2.2 nm)/Ag(flat)), Raman spectra were measured under the flow of 10 μM aqueous solution of 4-NP. Figure 6(a) shows the Raman spectra measured at times of 0, 2, 4, 6, 8, 10, 30, and 60 min. We can indeed observe the development of Raman peaks of 4-NP; the assignment of Raman spectrum of 4-NP can also be found in the literature.[39-41] These peaks must be due to 4-NP inside the nanogaps, indicating that 4-NP molecules can readily diffuse inside the P4VP film. The Raman intensity of 4-NP at 1327 cm^{-1} (denoted by an asterisk (*) in Figure 6(a)) *versus* the flow time of 4-NP is shown in Figure 6(b); the Raman intensities were normalized with respect to that of a silicon wafer at 520 cm^{-1}. Once again, the Raman peak became saturated within 10 min, as seen for 4-MBA in Figure 4(c). In Figure 6(b), the Raman peaks of P4VP at 999 cm^{-1} (denoted by a sharp (#) in Figure 6(a)), on the other hand, decrease in intensity, as also seen in Figure 4(c). Some P4VP molecules must have been displaced from the SERS-active sites by the diffusion of 4-NP.

The present experiments clearly suggest that P4VP is not a proper affixing layer for experiments supporting the PIEC model. The unfeasibility of the PIEC model was examined further using 1,4-PDI as the affixing layer. The reasoning behind this experiment is that 1,4-PDI has much stronger adsorption toward Ag than P4VP. 1,4-PDI is known to adsorb well on Ag *via* one of its two –NC groups, allowing new Ag nanoparticles to be able to adsorb on the pendent –NC group. In fact, no Raman peaks were identifiable at all when 1,4-PDI was assembled onto a flat Ag film. When Ag

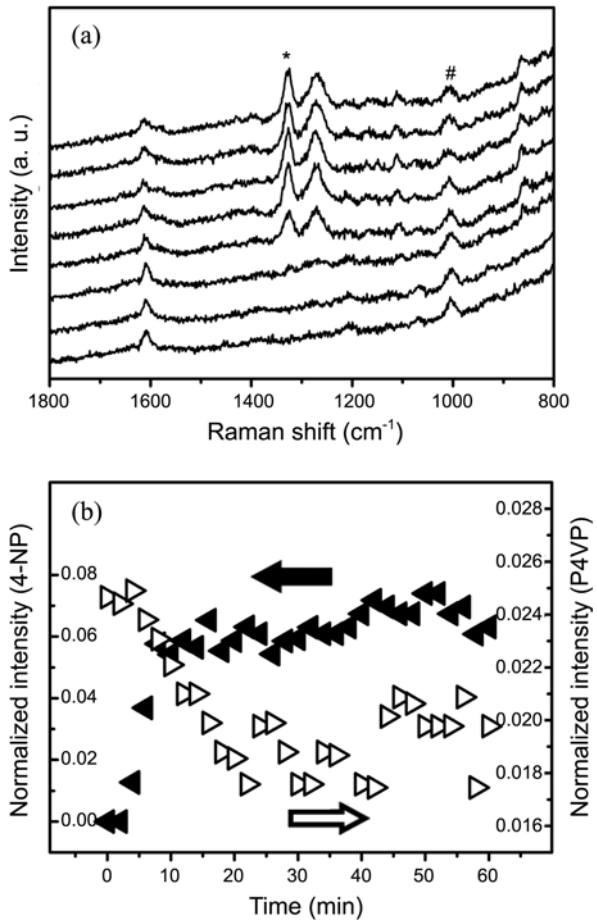

Figure 6. (a) Raman spectra measured as a function of time, i.e., at times of 0, 2, 4, 6, 8, 10, 30, and 60 min, under the flow of 10 μM aqueous solution of 4-NP through a capillary containing an Ag@P4VP (2.2 nm)/Ag(flat) substrate. (b) Intensity variation of 4-NP (denoted by an asterisk (*), filled triangles) and P4VP (denoted by a sharp (#), open triangles) *versus* the measurement time.

nanoparticles were adsorbed onto the pendent –NC group, this system could then be denoted as Ag@1,4-PDI/Ag(flat) and the Raman peaks of 1,4-PDI could be identified very distinctly (see the bottom spectrum of Figure 7(a)). We then carefully examined what happens when 10 μM 4-MBA solution is flowed over the Ag@1,4-PDI/Ag(flat) system. It should be noted that, on the one hand, the thickness of 1,4-PDI must be well below 2.2 nm and, on the other hand, 10 min must be a sufficient time for the probe molecule to adsorb on the upper Ag nanoparticles. At least within 10 min, no Raman peaks due to 4-MBA were identifiable at all, however, as can be seen in the top spectrum of Figure 7(a). This can be regarded as evidence of the unfeasibility of the PIEC model. Instead, we found that the second molecule can at least affect the surface potential of the Ag nanoparticles, letting the SERS peaks of 1,4-PDI shift in accordance with the electron- donating/electron-accepting capability of the second molecule to/from Ag, as illustrated in Figure 7(b). The NC stretching band of 1,4-PDI has red-shifted by as much as 3 cm^{-1} upon contact of the Ag nanoparticles with 4-MBA. This must be caused by electron donation from the

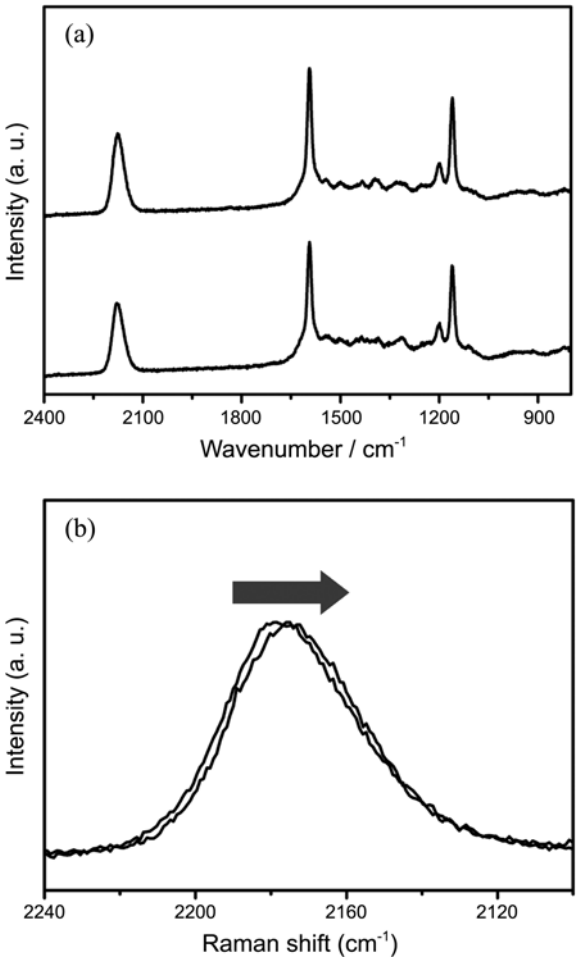

Figure 7. (a) SERS spectra of 1,4-PDI situated in the nanogaps between the Ag nanoparticles and the flat Ag substrate (Ag@1,4-PDI/Ag(flat)) measured in the flow of pure water (bottom) and 10 μM aqueous solution of 4-MBA (top). (b) Magnified view of the specific region of NC stretching band in (a).

sulfur atom of 4-MBA to the Ag nanoparticles.[42,43]

Summary and Conclusion

We have carried out a series of Raman spectral measurements to determine whether the PIEC model is appropriate. As in the original experiment, we first prepared P4VP films with different thicknesses (from 2.2 to 65 nm) on macroscopically smooth Ag substrates by spin-casting and then constructed a nanogap system by adsorbing 75-nm-sized Ag nanoparticles onto them to a surface coverage of 11 per μm^2. Without the help of Ag nanoparticles, no Raman signal could be detected at all, even for a 65-nm-thick P4VP film, while the P4VP signal was detectable even for a 2.2-nm-thick film in the presence of Ag nanoparticles. As the thickness of the P4VP film increased, however, the Raman signal decreased noticeably, becoming barely detectable when the gap distance reached ~10 nm. This suggests that the electromagnetic coupling of the surface plasmon of the Ag nanoparticles and the surface plasmon polariton of the underlying Ag film is effective only for ranges of a few nanometers. Anyhow, when foreign molecules such as 4-MBA were flowed over the Ag@P4VP/Ag(flat) system, we could witness the incremental appearance of the Raman peaks of 4-MBA, coupled with the gradual disappearance of the P4VP peaks. At a first glance, this observation appeared to support the PIEC model, but a careful examination led us to conclude that the phenomenon was simply due to the penetration of 4-MBA molecules into the gap sites originally occupied by P4VP. Much the same conclusion could be made even when 4-NP was used as a foreign molecule that should hardly be able to adsorb on the Ag nanoparticles. Accordingly, most of the Raman signal in a nanogap system is presumed to arise from molecules situated at the gap center, as reported in our earlier publication. In any case, we separately demonstrated in this work that although it is difficult to directly detect the foreign molecules that are adsorbed on the Ag nanoparticles, their effect on the surface charge (and thus the surface potential) of Ag nanoparticles can be seen from the shift of the NC stretching band of 1,4-PDI trapped in an Ag@1,4-PDI/Ag(flat) system.

Acknowledgments. This work was supported by National Research Foundation (NRF) of Korea grants funded by the Korean Government (MEST) (Grants 2007-0056334, 2012-0001352, 2012-0006225, and 2012008004).

References

1. Chang, R. K.; Furtak, T. E. *Surface Enhanced Raman Scattering*; Plenum Press: New York, 1982.
2. Nie, S.; Emory, S. R. *Science* **1997**, *275*, 1102.
3. Kneipp, K.; Wang, Y.; Kneipp, H.; Itzkan, I.; Dasari R. R.; Feld, M. S. *Phys. Rev. Lett.* **1996**, *76*, 2444.
4. Xu, H.; Bjerneld, E. J.; Käll, M.; Börjesson, L. *Phys. Rev. Lett.* **1999**, *83*, 4357.
5. Futamata, M.; Maruyama, Y.; Ishikawa, M. *Vib. Spectrosc.* **2002**, *30*, 17.
6. Vlčková, B.; Moskovits, M.; Pavel, I.; Šišková, K.; Sládková, M.; Šlouf, M. *Chem. Phys. Lett.* **2008**, *455*, 131.
7. Le Ru, E. C.; Blackie, E.; Meyer, M.; Etchegoin, P. G. *J. Phys. Chem. C* **2007**, *111*, 13794.
8. Chu, W.; LeBlanc, R. J.; Williams, C. T.; Kubota, J.; Zaera, F. *J. Phys. Chem. B* **2003**, *107*, 14365.
9. Doering, W. E.; Nie, S. *J. Phys. Chem. B* **2001**, *106*, 311.
10. Ni, J.; Lipert, R. J.; Dawson, G. B.; Porter, M. D. *Anal. Chem.* **1999**, *71*, 4903.
11. Kim, N. H.; Lee, S. J.; Kim, K. *Chem. Commun.* **2003**, 724.
12. Cao, P. G.; Gu, R. N.; Tian, Z. Q. *Langmuir* **2002**, *18*, 7609.
13. Moskovits, M. *Rev. Mod. Phys*. **1985**, *57*, 783.
14. Prodan, E.; Radloff, C.; Halas, N. J.; Nordlander, P. *Science* **2003**, *302*, 419.
15. Aravind, P. K.; Metiu, H. *J. Phys. Chem.* **1982**, *86*, 5076.
16. Jiang, J.; Bosnick, K.; Maillard, M.; Brus, L. *J. Phys. Chem. B* **2003**, *107*, 9964.
17. Kinnan, M. K.; Chumanov, G. *J. Phys. Chem. C* **2007**, *111*, 18010.
18. Hudson, S. D.; Chumanov, G. *J. Phys. Chem. C* **2008**, *112*, 19866.
19. Kim, K.; Shin, D.; Kim, K. L.; Shin, K. S. *Phys. Chem. Chem. Phys.* **2010**, *12*, 3747.
20. Mubeen, S.; Zhang, S.; Kim, N.; Lee, S.; Kramer, S.; Xu, H.; Moskovits, M. *Nano Lett.* **2012**, *12*, 2088.
21. Ikeda, K.; Suzuki, S.; Uosaki, K. *Nano Lett.* **2011**, *11*, 1716.
22. Lee, P. C.; Meisel, D. *J. Phys. Chem.* **1982**, *86*, 3391.

23. Kissinger, G.; Kissinger, W. *Phys. Stat. Sol. A* **1991**, *123*, 185.
24. Osman, M. A.; Keller, B. A. *Appl. Surf. Sci.* **1996**, *99*, 261.
25. See supplementary material at [URL will be inserted by AIP] for an AFM image of Ag film and a series of Raman spectra concerning the effect of 4-aminothiophenol or 4-mercaptophenol on Ag@P4VP/Ag(flat) system..
26. Pockrand, I. *Surface enhanced Raman vibrational studies at solid/gas interfaces*; Springer-Verlag: Berlin; New York, 1984.
27. Kim, K.; Kim, K. L.; Lee, S. J. *Chem. Phys. Lett.* **2005**, *403*, 77.
28. Kim, K.; Ryoo, H.; Lee, Y. M.; Shin, K. S. *J. Colloid. Interf. Sci.* **2010**, *342*, 479.
29. Ryoo, H.; Kim, K.; Shin, K. S. *Vib. Spectrosc.* **2010**, *53*, 158.
30. Kim, K.; Ryoo, H.; Shin, K. S. *Langmuir* **2010**, *26*, 10827.
31. Michota, A.; Bukowska, J. *J. Raman. Spectrosc.* **2003**, *34*, 21.
32. Osawa, M.; Matsuda, N.; Yoshii, K.; Uchida, I. *J. Phys. Chem.* **1994**, *98*, 12702.
33. Kim, K.; Yoon, J. K. *J. Phys. Chem. B* **2005**, *109*, 20731.
34. Kim, K.; Lee, H. B.; Yoon, J. K.; Shin, D.; Shin, K. S. *J. Phys. Chem. C* **2010**, *114*, 13589.
35. Lee, Y. M.; Kim, K.; Shin, K. S. *J. Phys. Chem. C* **2008**, *112*, 10715.
36. Lee, H. M.; Kim, M. S.; Kim, K. *Vib. Spectrosc.* **1994**, *6*, 205.
37. Fieldson, G. T.; Barbari, T. A. *Polymer* **1993**, *34*, 1146.
38. Pignatello, J. J.; Xing, B. S. *Environ. Sci. Technol.* **1996**, *30*, 1.
39. Ayora, M. J.; Ballesteros, L.; Perez, R.; Ruperez, A.; Laserna, J. J. *Anal. Chim. Acta* **1997**, *355*, 15.
40. Tanaka, Y.; Nakajima, A.; Watanabe, A.; Ohno, T.; Ozaki, Y. *Vib. Spectrosc.* **2004**, *34*, 157.
41. Ni, F.; Thomas, L.; Cotton, T. M. *Anal. Chem.* **1989**, *61*, 888.
42. Shin, D.; Kim, K.; Shin, K. S. *ChemPhysChem* **2010**, *11*, 83.
43. Kim, K.; Lee, J. W.; Shin, D. H.; Choi, J. Y.; Shin, K. S. *Analyst* **2012**, *137*, 1930.